

PACS numbers: 71.35.Lk; 42.50.Fx; 42.55.Px
DOI: 10.1070/QE2007v037n11ABEH013542

Influence of femtosecond superradiant pulses on spontaneous emission spectra of GaAs/AlGaAs heterostructures

P.P. Vasil'ev, H. Kan, T. Hiruma

Abstract. **The spectra of spontaneous emission accompanying the generation of femtosecond superradiant pulses in GaAs/AlGaAs heterostructures are studied. It is clearly demonstrated that spontaneous emission spectra of electron – hole pairs, which have been left in the semiconductor after the formation of a coherent collective e – h state, correspond to the strong overheating of carriers. This phenomenon can be explained by the effect of dynamic cooling and nonequilibrium condensation of collectively paired carriers at the bottoms of the bands during the superradiant emission, which was observed earlier.**

Keywords: *femtosecond pulses, superradiance, carrier heating, condensation.*

1. Introduction

Various processes of intraband dynamics of electrons and holes in semiconductor structures determine to a great extent the ultimate performance of ultrafast semiconductor lasers and amplifiers [1]. Many experimental and theoretical works have been devoted to the study of these processes for years [2 – 5]. It is generally accepted at present that the dynamic spectral hole burning and intraband carrier overheating influence decisively the nonlinear gain, the saturation energy, the maximum modulation frequency and other important characteristics of semiconductor lasers and amplifiers operating in various wavelength ranges.

The overheating of electrons and holes is caused mainly by stimulated emission when more cooler on average carriers leave the system. The energy of these carriers lies in a region located closer to the band bottoms compared to the average energies of the rest of the electrons and holes. The removal of colder carriers in this process results in the efficient heating of the remained electrons and holes. The overheating of them during lasing or pulse amplification was distinctly observed in pump – probe experiments with ultrashort pulses [2, 5] and during measurements of the spectral dynamics of the amplified spontaneous emission (ASE) [6]. It was found that the described processes had ultrashort durations and overheated carriers were thermolised at the picosecond time scale.

In addition, numerous experiments on the femtosecond pulse generation in semiconductor structures in a superradiant regime have been performed [7 – 11] in which cooperative recombination in a highly nonequilibrium high-density system of electrons and holes in bulk p – i – n GaAs/AlGaAs heterostructures has been studied at room temperature. It was shown that all the properties of cooperative emission can be adequately explained by the collective e – h pairing, the e – h condensation at the bottom of the bands, and the formation of a nonequilibrium coherent e – h BCS-like state. The average lifetime of this state is 200 – 400 fs. It was clearly demonstrated experimentally how electrons and holes move from the energy levels within the bands at the bottom of the conduction band and top of the valence band at the initial stage of the formation of a superradiant pulse [11].

The existence of the low-energy level of a bound collective electron – hole state near the energy gap was proved in [12]. It was also found that in a strong degenerate system the critical condensation temperature is determined by the Fermi energy rather than by the order parameter. The critical temperature can exceed 300 K at electron – hole densities about 6×10^{18} cm^{-3}. The radiative recombination of the collective state of condensed electron – hole pairs occurs in the form of a high-power femtosecond emission pulse with the lowest possible photon energy.

It is obvious that if a large number of the coldest electrons and holes are removed from the system, the remained carriers will be overheated for some time. Such a dynamic overheating of electrons and holes can be found by analysing their spontaneous emission. Indeed, the electron (hole) Fermi distribution depends on temperature, broadening with increasing temperature. This broadening leads to the broadening of spontaneous emission line with temperature. At the same time, the spontaneous amplification line should shift to the red due to the temperature dependence of the band gap.

This work is devoted to the study of the spectra of spontaneous emission accompanying femtosecond superradiant pulses. Both time-averaged optical spectra and time-resolved spectra using a streak camera are studied. It is shown that the dynamic overheating of electrons and holes does happen in the system.

P.P. Vasil'ev P.N. Lebedev Physics Institute, Leninsky prosp. 53, 119991 Moscow, Russia; e-mail: peter@sci.lebedev.ru;
H. Kan, T. Hiruma Central Research Lab, Hamamatsu Photonics K.K., 5000 Hirakuchi, Hamamatsu City, 434-8601 Japan

Received 19 February 2007
Kvantovaya Elektronika **37** (11) 1001 – 1005 (2007)
Translated by P.P. Vasil'ev

2. Experiment

We studied bulk p–i–n GaAs/AlGaAs double heterostructures, which were very similar to those described earlier [7–11]. The heterostructures were grown by the MOCVD technique on n-GaAs substrates. The active layer consists of an intrinsic 0.1–0.2-μm thick GaAs. A 5–6-μm wide mesa structure was etched in the upper heavily doped p-GaAs layer. Some structures had tapered optical waveguides with a width increasing along the structure axis from 5 to 20–40 μm. It was done in order to increase the intensity of the ASE from the edge of the structure.

The semiconductor structures were photolithographically divided into three sections along the axis of the cavity axis. Two of them, which were used as amplifiers and had a common electrical contact, were located at the chip ends. They were pumped by current pulses with amplitudes varied from 500 to 800 mA. The repetition rate of current pulses was changed from 10 Hz to 40 MHz depending on the detection technique. The middle section of the laser structure was connected to a dc voltage source. Reverse voltages up to −10 V were applied to this section.

We measured both standard time-averaged and time-resolved spectra of ASE and superradiant cooperative emission from the edge of the structures. Averaged optical spectra were measured with an ANDO AQ6315A optical spectrum analyser with a resolution of 0.05 nm.

Time-resolved optical spectra were studied as follows. The emission from a laser structure was collimated by a lens on a 600-lines mm^{-1} diffraction grating. The light diffracted to the third diffraction order was focused by a lens with a focal distance of 18 cm on an entrance slit of a streak camera. The ultimate single-shot time resolution of the camera was about 1.5 ps. Time-resolved optical spectra of the emission was displayed on the streak camera screen. Images from the screen were read off with a CCD camera and analysed with a personal computer. The linearity and intensity dynamic range of the camera were controlled by special optical filters. The streak speed was calibrated by a time delay of femtosecond pulses in a quartz plate of the known length. This measurement technique has been widely used for studies of the spectral dynamics of ultrafast semiconductor lasers [1].

By changing the pump conditions of the laser structures under study, different lasing regimes can be obtained, including pulsed lasing, ASE, and superradiant pulses. Figure 1 shows typical time-resolved optical spectra of superradiant pulses and ASE from one of the structures. The amplitudes of current pulses and the reverse bias are the same for both cases, but the electrical pulse width in Fig. 1b is shorter by about 0.1 ns. Both pictures show that the emission starts from spontaneous emission with a broad spectrum. A powerful superradiant pulse appears as a bright spot approximately within 2 ns after the beginning (Fig. 1a). It has the femtosecond duration and the minimum possible photon energy [7–10]. The visible duration of the superradiant pulse in Fig. 1 considerably exceeds its actual duration due to the chosen intensity of the image and poor time resolution of the streak camera at the slow (nanosecond) streak speed. The spontaneous emission intensity exhibits a distinct dip during the superradiant pulse generation (see details in [11]). The superradiant pulse is not formed upon a slight change in the pump pulse duration. A long nanosecond ASE pulse is observed at the output of the structure (Fig. 1b).

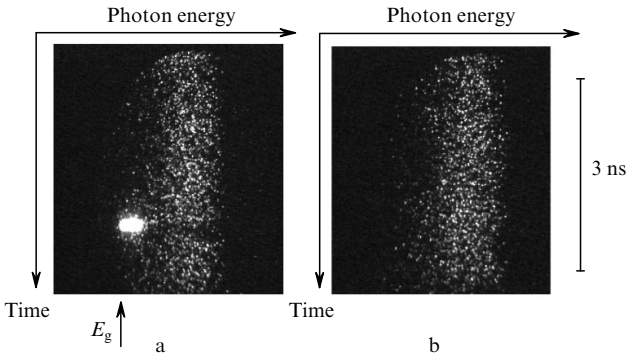

Figure 1. Typical time-resolved spectra of spontaneous emission and superradiant pulse (a) and ASE (b); E_g is the energy of the band gap. Figure 1a shows a dip in the spontaneous emission spectrum during the formation of the superradiant pulse.

Unlike our previous papers, in which characteristics of superradiant pulses themselves were studied, we investigated here the spontaneous emission accompanying femtosecond superradiant pulses. Due to technical limitations, it was impossible to measure optical bandwidths with resolution better than 1 nm using the time-resolved detection with the streak camera. Accurate spectral measurements were carried out by using the optical spectrum analyser.

Figure 2 shows ASE spectra detected by the streak camera before and after the generation of the superradiant pulse. One can see that the ASE spectrum detected after the superradiant pulse is wider than the spectrum detected before the pulse. This implies that electrons and holes left after the collective state recombination have a higher temperature than at the beginning of the pump pulse (see Section 3). This effect was observed in averaged ASE spectra as well.

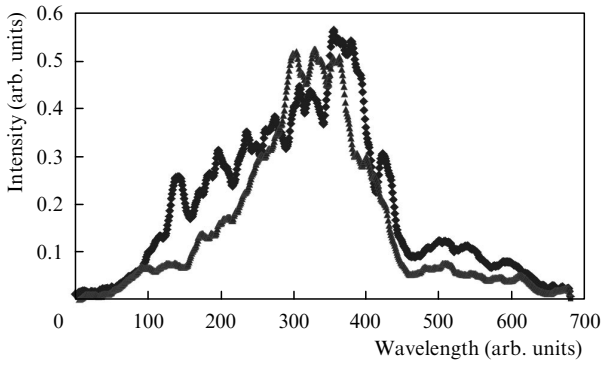

Figure 2. Amplified spontaneous spectra just before (▲) and after (◆) the generation of a cooperative emission pulse.

Figure 3 shows typical averaged ASE spectra with and without the superradiant pulse, which correspond to the two cases shown in Fig. 1. Because the spectral energy and peak power of superradiant pulses considerably exceeds those for ASE, the spectrum of the superradiant pulse is saturated at the given vertical scale of the device.

An important feature should be noted. Both spectra in Fig. 3 were taken at the same amplitudes of the pump current and the reverse bias at the absorber of the structure.

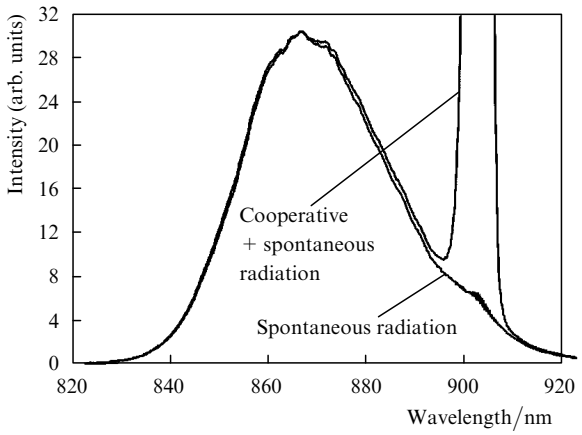

Figure 3. Time-averaged spectra corresponding to pulses shown in Fig. 1. The scale was chosen to make the maxima of the spontaneous emission intensity coincident.

The only difference is that in the case of the superradiant pulse generation the duration of the current pulse was slightly longer. The duration of the current pulse and consequently the injected electron–hole density were enough for the formation of the coherent collective state [13, 14]. The carrier density at a slightly shorter duration of the current pulse did not achieve the required value and the superradiant pulse was not formed.

One can see from Fig. 3 that the ASE spectrum in the presence of the superradiant pulse is slightly broader and is slightly shifted to the red compared to the spectrum in the absence of this pulse. The effect is not large compared to the difference in the instantaneous spectra (see Fig. 2); however, it has been clearly observed in many laser structures at different pump conditions.

Figure 4 shows the full width at half-maximum (FWHM) of the ASE spectra in both cases obtained in a number of measurements. The ASE spectra were always broader in the superradiant pulse generation regime. The difference $\Delta\lambda$ of the widths of the spectra is shown in Fig. 5. The mean value of $\Delta\lambda$ is 0.52 nm, the largest measured value achieving 1 nm.

Note in conclusion that we have found experimentally that both average and instantaneous ASE spectra broaden

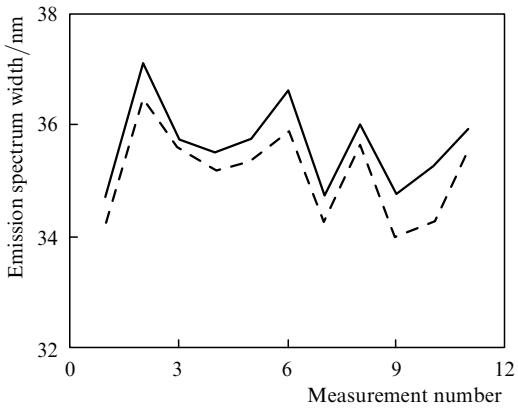

Figure 4. Full width at half-maximum of averaged ASE spectra just before (dashed line) and after (solid line) the generation of the superradiant pulse.

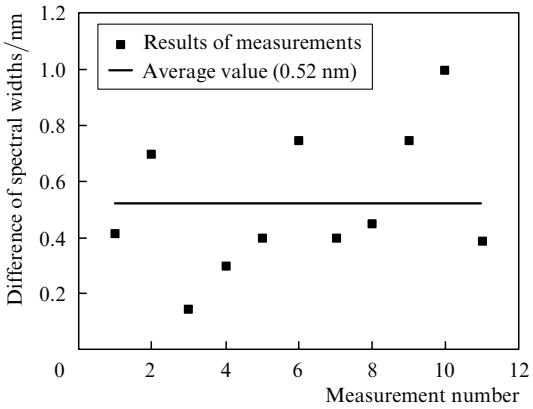

Figure 5. Difference of the bandwidths of the spectra presented in Fig. 4.

when superradiant emission pulses are generated. Let us show now that this effect is caused by the overheating of electrons and holes within the bands.

3. Discussion

As we have noted already, both curves in Fig. 3 were obtained at virtually the same pump current and reverse bias. Thus, the change in the ASE spectrum width cannot be determined by the difference in the pump conditions but can be caused only by the presence of the femtosecond superradiant pulse. Because the superradiant pulse is formed due to the recombination of the cooperative state of bound electron–hole pairs with the minimum possible energy, a large number of the coldest electrons and holes leave the ensemble within 200–400 fs. This means that the remained electrons and holes will have an additional energy compared to the normal condition before the pulse emission or compared to the case when the superradiant pulse is not formed.

The situation under study is quite similar to the carrier overheating upon lasing or pulse amplification in semiconductor amplifiers described in Introduction. A substantial difference is that the optical gain maximum in these regimes is shifted from the bottom inside the bands by approximately kT. Therefore, electrons and holes, which occupy energy levels inside the bands, take part in stimulated emission transitions. In our case of the superradiant emission, colder electron–hole pairs, which are at the very bottom of the band gap, leave the system. Therefore, the carrier overheating should manifest itself more strongly.

Now we will show that a change in the carrier temperature can be detected by a change in the ASE spectra measured from the edge of the semiconductor structure. Strictly speaking, this emission spectrum is not a true ASE spectrum due to a spectral distortions during amplification in the optically thick semiconductor medium. However, it was shown earlier [15] that the ASE spectrum $I(\omega)$ observed from the end of a sample of length L and originating from the spontaneous emission spectrum $I_{sp}(\omega)$ distributed uniformly along the sample length is

$$I(\omega) = \frac{I_{sp}(\omega)\{\exp[(G(\omega) - \alpha_i)L] - 1\}}{G(\omega) - \alpha_i}, \quad (1)$$

where $G(\omega)$ is the modal optical gain and α_i is the internal nonresonant loss. The modal gain is a product of the

material gain and the optical confinement factor. The spontaneous emission intensity depends, in particular, on the electron and hole Fermi level separation ΔE_F upon current injection through the structure [16]

$$I_{sp}(\omega, \Delta E_F) = \frac{n^2(\hbar\omega)^2}{\pi^2\hbar^3c^2}\,\alpha(\omega)\exp\left(\frac{\Delta E_F - \hbar\omega}{kT}\right), \qquad (2)$$

where n is the refractive index, c is the velocity of light, $\alpha(\omega)$ is the resonant absorption, k is the Boltzman constant, T is temperature. The material optical gain has the from [16]

$$g(\omega, \Delta E_F) = \frac{\pi^2\hbar^3c^2}{n^2}\,\frac{1}{(\hbar\omega)^2}$$

$$\times\left\{1 - \exp\left(\frac{\Delta E_F - \hbar\omega}{kT}\right)\right\} I_{sp}(\omega, \Delta E_F). \qquad (3)$$

The resonant absorption $\alpha(\omega)$ in (2) in undoped GaAs can be approximated by an analytic function consisting of a sum of two parts representing the transitions in the continuum and exciton spectral regions [17]. The latter is negligible in bulk GaAs at room temperature. The contribution of interband transitions near the energy of the band gap E_g is [17]

$$\alpha(E') = \frac{A\exp\left[r(E')\right]}{1 + \exp\left(-E'/E_{s1}\right)} \qquad (4)$$

with $r(E') = r_1E' + r_2E'^2 + r_3E'^3$, and $E' = \hbar\omega - E_g$. The parameters of the approximation r_1, r_2, r_3 can be found [17]. By calculating the absorption coefficient, the gain, and the true spontaneous emission intensity I_{sp} from (2)–(4), we can estimate the ASE intensity $I(\omega)$ from the end of a sample and compare it with the experimental data.

This procedure is well known and has been used many times before (see, for instance, [15, 16] and references therein). To prove the validity of this procedure for our structures, we calculated wavelength dependences of the ASE intensity (Fig. 6). One can see that the experimental data are fitted well by the calculated curve over the entire range except the curve wings. This is explained as follows. The dipole matrix element of the interband transition in calculations by (1)–(4) was assumed constant. However, strictly speaking, it depends on the transition energy, which should be taken into account in more rigorous calculations, but this is beyond the scope of our paper.

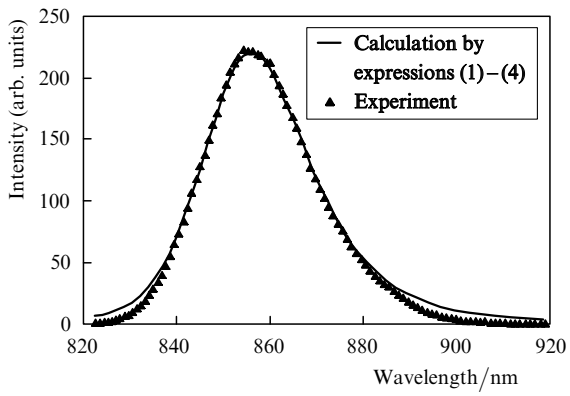

Figure 6. Approximation of the ASE spectrum.

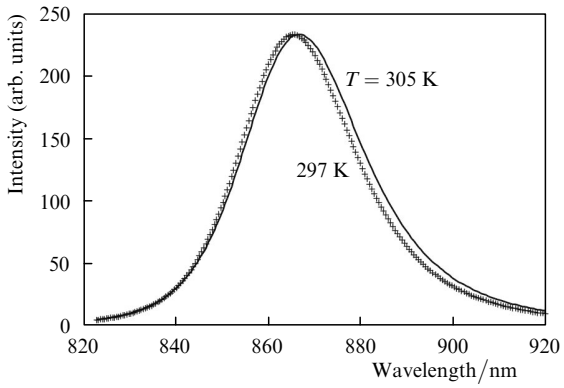

Figure 7. Calculated ASE spectra for two lattice temperatures.

Figure 7 illustrates how the calculated ASE spectrum of from the edge of the structure depends on temperature. We calculated the function $I(\lambda)$ for temperatures $T = 297$ and 305 K. One can see that a small increase in the temperature results in the broadening of the spectrum and a small red shift which was observed in our experiments.

Theoretical calculations of the spectral line broadening can be used for qualitative estimates of the temperature rise during the dynamical carrier overheating. Strictly speaking, the measured average spontaneous line broadening $\Delta\lambda$ shown in Fig. 5 depends on a ratio of the intensities of spontaneous emission before and after the generation of superradiant pulses (see Fig. 1a). This ratio at different pump regimes in experiments is in the range from 3 : 1 to 4 : 1. Taking into account this fact and using the data in Fig. 5, we can conclude that the electron–hole temperature after the emission of the cooperative pulse is higher by about 5–10 °C than that before its emission. This is the value of the carrier temperature that was averaged over approximately 1 ns. The carrier overheating is strong because the temperature change could be detected for such a long time interval. Indeed, it is well known [1–6] that the intraband carrier thermalisation occurs during an ultrashort time, a typical value being around 1 ps. Therefore, the electron–hole temperature should be equal to the lattice temperature after 10–20 ps. The spontaneous emission, which was detected after the carrier thermalisation, will strongly reduce overheating, which is measured at a long (nanosecond) time scale. The average temperature rise by 5–10 degrees, detected during 1 ns, implies that the instantaneous carrier overheating immediately after the superradiant pulse generation can exceed a few hundred degrees.

Thus, we believe that the temperature increase observed in experiments is caused only by the generation of the high-power ultrashort cooperative emission pulse. In our opinion, this pulse is generated due to the radiative recombination of a coherent ensemble of collectively paired electrons and holes that are condensed at the bottom of the bands. These pairs are in the ground state with the lowest possible energy. The decay of the coherent ensemble within hundred femtosecond leads to a fast disappearance of a large number of the coldest carriers. As a result, the rest of the unbound electrons and holes prove to be strongly overheated.

4. Conclusions

We have studied ASE spectra accompanying the generation of femtosecond superradiant pulses in GaAs/AlGaAs

heterostructures. We have experimentally demonstrated that the ASE spectra are broader by 0.5 – 1 nm after the emission of a cooperative pulse than those without the generation of this pulse. This fact corresponds to the heating of electrons and holes remaining in the ensemble after the escape of colder carriers [7 – 14].

The average temperature increase has been estimated by approximating the observed spectra. The average carrier overheating during approximately 1 ns after the emission of the femtosecond superradiant pulse was 5 – 10 degrees. This value corresponds to the dynamic temperature rise of electrons during the very first moments after the emission of the cooperative pulse by over a few hundreds of degrees.

Acknowledgements. The authors thank I.V. Smetanin for helpful discussions. The work was partially supported by the Russian Foundation for Basic Research (Grant No. 06-02-16173a) and 'The Leading Research Schools' (Grant No. NSh-6055.2006.2).

References

1. Vasil'ev P. *Ultrafast Diode Lasers: Fundamentals and Applications* (Norwood: Artech House, 1995).
2. Kesler M.P., Ippen E.P. *Appl. Phys. Lett.,* **51**, 1765 (1987).
3. Gomatam B.N., DeFonzo A.P. *IEEE J. Quantum Electron*., **26**, 1689 (1990).
4. Uskov A., Mork J., Mark J. *IEEE Photon. Tech. Lett*., **4**, 443 (1992).
5. Kaiser J., Fischer I., Elsasser W., Gehrig E., Hess O. *IEEE J. Quantum Electron*., **42**, 363 (2006).
6. Nido M., Suzuki A. *Appl. Phys. Lett*., **64**, 681 (1994).
7. Vasil'ev P.P., Kan H., Ohta H., Hiruma T. *Zh. Eksp. Teor. Fiz*., **120**, 1486 (2001) [*JETP*, **93**, 1288 (2001)].
8. Vasil'ev P.P., Kan H., Ohta H., Hiruma T. *Phys. Rev. B*, **64**, 195209 (2001).
9. Vasil'ev P.P., Kan H., Ohta H., Hiruma T. *Zh. Eksp. Teor. Fiz.,* **123**, 310 (2003).
10. Vasil'ev P.P. *Phys. Stat. Sol. B*, **241**, 1251 (2004).
11. Vasil'ev P.P. *Pis'ma Zh. Eksp. Teor. Fiz*., **82**, 129 (2005) [*JETP Lett*., **82**, 115 (2005)].
12. Vasil'ev P.P., Smetanin I.V. *Phys Rev. B*, **74**, 125206 (2006).
13. Vasil'ev P.P., Kan H., Ohta H., Hiruma T. *Kvantovaya Elektron*., **31**, 870 (2001) [*Quantum Electron*., **31**, 870 (2001)].
14. Vasil'ev P.P., Kan H., Ohta H., Hiruma T. *Kvantovaya Elektron*., **32**, 1105 (2002) [*Quantum Electron*., **32**, 1105 (2002)].
15. Lewis G.M., Smowton P.M., Thomson J.D., et al. *Appl. Phys. Lett*., **80**, 1 (2002).
16. Blood P., Kucharska A.I., Jacobs J.P., et al. *J. Appl. Phys*., **70**, 1144 (1991).
17. Reinhart F.K. *J. Appl. Phys*., **97**, 123534 (2005).